2013 European Control Conference (ECC)
July 17-19, 2013, Zürich, Switzerland.

A Novel Adaptive Unscented Kalman Filter Attitude Estimation and Control Systems for 3U Nanosatellite

Junquan Li; Mark A. Post; Regina Lee
York University, 4700 Keele Street Toronto, Ontario M3J 1P3, Canada

***Abstract*— A novel adaptive unscented Kalman filter (AUKF) based estimation algorithm is proposed for a 3U Cubsat. This small satellite employs a three axis magnetometer and three MEMS gyroscopes as well as three magnetic torque rods and one reaction wheel on the pitch axis. Unlike the existing UKF, in this paper, an $n+1$ sigma set is used to estimate the nanosatellite attitude instead of $2n+1$ sigma points as in a conventional UKF. Numerical Simulation results validate the performance of the proposed adaptive Kalman filter. There is no need for linearization of the nonlinear dynamics of the system. The estimated result tracks satellite attitude during the damping and stable control stages. Euler angles, gyro bias, and angular velocity of the satellite are estimated using this proposed AUKF with good convergence time and estimation accuracy.**

I. INTRODUCTION

During the past decades, nanosatellites have became a leading platform for low cost space-borne experiments. CubeSats have a short development time and frequent launch opportunities, providing easy access to space by using a common platform and sharing launches with larger spacecraft. By Spetember 2009, at least 60 CubeSats had been launched successfully into space. A 1U CubeSat with a size of $10cm \times 10cm \times 10cm$ can not carry large or high-powered payloads, but 3U CubeSats with a size of $30cm \times 10cm \times 10cm$ are now being used to carry scientific payloads. Attitude determination and control (ADCS) is one of the most important parts of the operation of nanosatellites [1]. In this research, various attitude determination and control methods are evaluated through simulations. Pure Magnetic attitude control provides robustness, light weight, low power consumption and cost efficiency, and is commonly used for nanosatellites. A pure magnetic control system includes a magnetometer and three magnetic torque rods. Interactions between the three magnetic dipole moments generated by the rods and the Earth's magnetic field produce a torque that rotates the satellite [2]. However, the attitude pointing accuracy is within 5 degrees. In this research, we compare control systems using pure magnetic methods with hybrid magnetic control methods. The hybrid magnetic control system includes a magnetometer, three magnetic torque rods and one flywheel, resulting in better attitude accuracy of within 0.005 degree. In this paper, the simulation results of pure and hybrid magnetic control systems are verified and compared, including the detumbling control and nadir pointing control of a satellite. Magnetic torquing research has mainly been focused on three-axis attitude control of a non-spinning small satellite. Magnetic torquers have been very popular for use with linear and nonlinear control techniques [3]. Nonlinear control includes Lyapunov-based control [4], sliding mode control [5], periodic linear quadratic regulation control [6] and so on. Both linear and nonlinear controllers need tuning. The nonlinear adaptive fuzzy sliding mode controller used in this paper has proven to be more robust to model uncertainty and actuator faults than linear controllers.

Satellite attitude determination with nonlinear filters has been studied by many researchers. In the reference [7], many nonlinear filtering methods for spacecraft attitude determination have been surveyed. The Unscented Kalman filter (UKF) is one of the most popular nonlinear filters for ACS systems [8] [9] [10]. Due to the use of statistical estimation in the UKF, the Jacobians and Hessians do not need to be calculated, and it does not require linearization as in the Extended Kalman Filter. The prior statistical distributions of the state variables are encapsulated with sigma points (state space samples) and transformed to posterior distributions using a system model. Making appropriate assumptions of the prior covariances is key to achieving good estimation results, but most UKF implementations assume that the statistics and covariances remain constant. One way to overcome this limitation is to use an adaptive algorithm for the UKF statistics [11]. The Unscented Kalman filter has been often used for parameter estimation because of its ability to handle nonlinear systems very well [12]. The formulation for parameter estimation with a UKF includes the computation of weights, the establishment of sigma points, the prediction of the mean and covariance of both states and measurements, the prediction of cross covariance, the gain calculation, and the state update step. However, the computational load is proportional to the number of sigma points. There are three common sets of sigma points used in the literature: the symmetric set, the reduced set, and the spherical set. In a recent publication [13], a new minimum sigma set with equal size to the reduced set but better high-order performance is proposed and applied to localization and map building. In our earlier research paper [14], we applied this new sigma set which uses $n+1$ sigma points to the adaptive unscented Kalman filter to achieve higher performance in comparison to the symmetric set which uses $2n+1$ sigma points. In this paper, the proposed novel adaptive unscented Kalman filter is used to estimate the angular velocity, attitude, and gyro

MITACS PDF, Department of Space Science and Engineering; junquanl@yorku.ca.
PhD Candidate, Department of Earth and Space Engineering; markpost@yorku.ca.
Assistant Professor, Department of Earth and Space Engineering; reginal@yorku.ca.

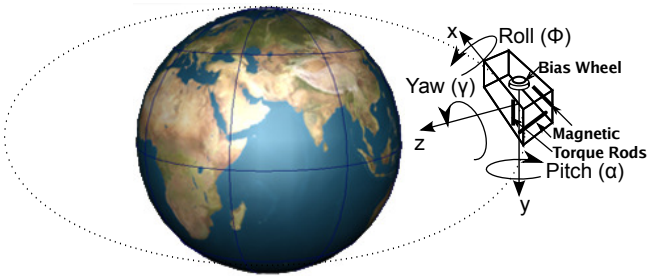

Fig. 1. Geometric configuration of a 3U CubeSat under developed in York University

drift of the system.

The organization of this paper proceeds as follows: First, the nonlinear system model and measurement model are presented. Then, the attitude control system using pure magnetic control and hybrid magnetic control is addressed. Third, the novel adaptive Unscented Kalman Filter is presented. Finally, the performance of the proposed ADCS is demonstrated for damping and stable modes of the satellite.

II. Mathematical Model of the Nanosatellite

The spacecraft is modeled as a rigid body with reaction wheels that provide torques about three mutually perpendicular axes that define a body-fixed frame *B* (shown in Fig. 1). The equations of motion are given by

$$\hat{J}\dot{\omega} = -\omega^{\times}(J_s\omega + A_i J_w \Omega) + A_i\tau_w + \tau_m + d \quad (1)$$

$$\dot{q} = \frac{1}{2}\begin{pmatrix} q_4 I_{3\times 3} + \bar{q}^{\times} \\ -\bar{q}^T \end{pmatrix}\omega \equiv \frac{1}{2}A(q)\omega \quad (2)$$

$$\begin{bmatrix}\dot{\psi}\\ \dot{\alpha}\\ \dot{\gamma}\end{bmatrix} = \begin{bmatrix}1 & sin(\psi)tan(\alpha) & cos(\psi)tan(\alpha)\\ 0 & cos(\psi) & -sin(\psi)\\ 0 & sin(\psi/cos(\alpha)) & cos(\psi)/cos(\alpha)\end{bmatrix}\omega \quad (3)$$

where $\omega = (\omega_1, \omega_2, \omega_3)^T$ is the angular velocity of the spacecraft with respect to an inertial frame *I* and expressed in the body frame *B*, Ω is the angular velocity of the reaction wheel, $J_s \in R^{3\times 3}$ is the inertia matrix of the spacecraft, $\hat{J} = J_s - A_i J_w A_i^T$; $\tau \in R^3$ is the torque control, A_i is the 3×4 or 3×3 (depending on the layout and the number of reaction wheels) matrix whose columns represent the influence of each reaction wheel on the angular acceleration of the satellite, $d \in R^3$ is the bounded external disturbance (included Solar Radiation Pressure Disturbance, Aerodynamic drag, and Gravity Gradient Torque), $x^{\times} \in R^{3\times 3}$ represents the cross product operator for a vector $x = (x_1, x_2, x_3)^T$ given as

$$x^{\times} = \begin{pmatrix} 0 & -x_3 & x_2 \\ x_3 & 0 & -x_1 \\ -x_2 & x_1 & 0 \end{pmatrix} \quad (4)$$

and the unit quaternion $q = (\bar{q}^T, q_4)^T = (q_1, q_2, q_3, q_4)^T$ represents the attitude orientation of a rigid spacecraft in the body frame *B* with respect to the inertial frame *I*, which is defined by

$$\bar{q} = (q_1, q_2, q_3)^T = e\sin(\theta/2), \quad q_4 = \cos(\theta/2) \quad (5)$$

where e is the Euler axis, and θ is the Euler angle. ψ is the roll angle about the x-axis. α is the pitch angle about the y-axis. γ is the yaw about the z-axis. The unit quaternion q satisfies the constraint

$$q^T q = 1 \quad (6)$$

The torques generated by the reaction wheels τ are given by

$$\tau_w = J_w(\dot{\Omega} + A_i^T\dot{\omega}) \quad (7)$$

Remark 1: For pure magnetic control, there is no wheel. $\Omega = 0$. $\hat{J} = J_s$. For hybrid magnetic control in this research, there is only one wheel that rotates about the y-axis.

Remark 2: There are two stages of the satellite operation. First, the satellite is separated from the launcher with a large angular velocity. This stage is damping mode. In this stage, pure magnetic control is used for the ACS. the quaternion based attitude kinematics are used for the ADS. The attitude determination system only estimates the angular velocity and gyro drift. Second, the satellite is stabilized by the adaptive fuzzy sliding mode controller for nadir pointing. The quaternion based nonlinear equations of motion are used for the ACS. For this stage, the satellite is required to keep pointing accuracy. the Euler angle attitude kinematics are used for the ADS. The estimated states are roll, pitch, and yaw.

III. Measurement Sensor Model of the Nanosatellite

A. The Magnetometer Model

The magnetic field vector is obtained in the orbit reference frame [10]:

$$B_1 = \frac{M_e}{{r_0}^3}[cos(\omega_0 t)(cos(\varepsilon)sin(i) - sin(\varepsilon)cos(i)cos(\omega_e t)) - sin(\omega_0 t)sin(\varepsilon)sin(\omega_e t)] \quad (8)$$

$$B_2 = -\frac{M_e}{{r_0}^3}[(cos(\varepsilon)cos(i) + sin(\varepsilon)sin(i)cos(\omega_e t)) \quad (9)$$

$$B_3 = \frac{2M_e}{{r_0}^3}[sin(\omega_0 t)(cos(\varepsilon)sin(i) - sin(\varepsilon)cos(i)cos(\omega_e t)) - 2sin(\omega_0 t)sin(\varepsilon)sin(\omega_e t)] \quad (10)$$

where, ω_0 is the angular velocity of the orbit with respect to the inertial frame. r_0 is the distance from the center of the satellite to the center of the Earth. i is the orbit inclination. ε is the magnetic dipole tilt. ω_e is the spin rate of the Earth. M_e is the magnetic dipole moment of Earth.

The magnetometer model should be:

$$H(\psi, \alpha, \gamma, t) = C_k\begin{bmatrix}B_1\\ B_2\\ B_3\end{bmatrix} + \eta_m \quad (11)$$

where C_k is the direction cosine matrix in terms of Euler Angles [10]. η_m is the zero mean Gaussian white noise of the magnetometer.

B. The Rate Gyro Model

The angular velocity is measured from three rate gyros. A well-known model for the angular velocity measurement is given by

$$\omega_g = \omega + b_g + \eta_g \tag{12}$$

where $\eta_g \in R^3$ is the output of the gyro, and ω is the real angular rate of the gyro, η_g and η_f are independent Gaussian white noise with zero mean and standard deviation. b_g is the random drift. k_f is a constant number.

$$\dot{b}_g = -k_f b_g + \eta_f \tag{13}$$

IV. Magnetic Attitude Control Systems

A lot of good research into magnetic attitude control systems for satellites has been done [15] [16]. Three Magnetic rods are used as actuators in this research. During the detumbling phases, the B-dot algorithm is the most popular control law. Once the angular velocity is low, we can use a modified magnetic control law based on [17]. Most of the references for magnetic attitude control only consider the Gravity Gradient torques as disturbances. In this research, all of the possible disturbances are included. The ADS is inactive in the detumbling phase, and is active in the stable nadir pointing phase. For the simulation case 1 in this paper, the desired control torque, $\vec{\tau_m}$ (torque is not possible in a vector parallel to $\vec{B}$) can be written as

$$\vec{\tau_m} = \vec{M} \times \vec{B} \tag{14}$$

where $\vec{B}$ is the local geomagnetic field vector, and M is the dipole moment of the magnetic coils. In the first ACS phase, $M = H\bar{\omega}_e \times B$. In the second ACS phase, $M = H\bar{\omega}_e \times B + A\bar{q}_e \times B$. For the nadir pointing phase, three magnetic rods and one flying wheel are used as actuators. The nonlinear adaptive fuzzy sliding controller used for this phase is given by [18]

$$\tau_{AFSMC} = -k_1 S - \theta^T \xi - \kappa tanh(\frac{3K_u \kappa S}{\epsilon}) \tag{15}$$

$$\dot{\theta} = \alpha S \xi \tag{16}$$

$$S = \dot{\bar{q}}_e + K\bar{q}_e \tag{17}$$

The desired orientation is $q_d = (\bar{q}_d^T, q_{4d})^T$, and the tracking errors are defined as

$$\bar{q}_e = q_{4d}\bar{q} - q_4\bar{q}_d + \bar{q}^{\times}\bar{q}_d \tag{18}$$

$$q_{4e} = q_{4d}q_4 + \bar{q}_d^T\bar{q} \tag{19}$$

where S is the sliding surface, and α, κ, ϵ are positive constant numbers. ξ is built using fuzzy membership functions. $H_r = \theta^T\xi$ is the estimation of the nonlinear dynamics function by a fuzzy logic system.

For the simulation case 2, the magnetic control law uses

$$M = \frac{\tau_{ap} \times B}{\|B^2\|} \tag{20}$$

$$\vec{\tau_m} = \vec{M} \times \vec{B} = \frac{\tau_{AFSMC} \times B}{\|B^2\|} \times B \tag{21}$$

V. Novel Adaptive Unscented Kalman Filter

For highly non-linear satellite attitude control systems with large disturbances, the adaptive unscented Kalman filter (AUKF) is a good choice for the reasons stated above. The formulation for parameter estimation with the AUKF is shown as follows:

Consider the discrete nonlinear system:

$$X_{k+1} = f(X_k, u_k, k) + \eta_{sk} \tag{22}$$

$$Z_{K+1} = h(X_{k+1}, u_{k+1}, k+1) + \eta_{ok+1} \tag{23}$$

where $X_k \in R_L$ is the state vector, $Z_k \in R_M$ is the output vector at time k, u_k is the control input at time k, d_k is the disturbance at time k, η_{sk} is the white noise with a mean of q_k and covariance Q_k, and η_{ok} is the white noise with a mean of r_k and covariance R_k.

The conventional UKF [10] is based on the determination of $2n+1$ sigma points. The sigma points are obtained by

$$\hat{\chi}_0 = \hat{x}_{k+1} \tag{24}$$

$$\hat{\chi}_{i,k+1} = \hat{x}_{k+1} + \sqrt{(n+\kappa)\,(P_{(k+1)i} + Q_k)}, \forall i = 1, 2, ..., n \tag{25}$$

$$\hat{\chi}_{i,k+q} = \hat{x}_{k+1} - \sqrt{(n+\kappa)\;\;(P_{(k+1)i} + Q_k)}, \forall i = n+1, ..., 2n \tag{26}$$

where $\hat{\chi}_{i,k}$ are sigma points, n is the state number and κ is the scaling parameter. The next step is prediction. Each point is run through the nonlinear system model to yield a set of transformed points

$$\hat{\chi}_{i,k|k+1} = f(\hat{\chi}_{i,k+1}) \tag{27}$$

The transformed values are utilized for gaining the predicted mean and covariance

$$\hat{x}_{k|k+1} = \sum_{i=0}^{2n} W_i^m\;\hat{\chi}_{i,k|k+1} \tag{28}$$

$$P_{k|k+1} = \sum_{i=0}^{2n} W_i^c\;(\hat{\chi}_{i,k|k+1} - \hat{x}_{k|k+1})(\hat{\chi}_{i,k|k+1} - \hat{x}_{k|k+1})^T \tag{29}$$

$$W_i{}^m = \frac{\kappa}{n+\kappa} \tag{30}$$

$$W_i{}^c = \frac{1}{2\,(n+\kappa)} \tag{31}$$

The predicted observation vector $\bar{y}_{k|k+1}$ and its predicted covariance P_{yy} are defined by

$$Y_{i,k|k+1} = h(\hat{\chi}_{i,k|k+1}, k+1) \tag{32}$$

$$\bar{y}_{k|k+1} = \sum_{i=0}^{2n} W_i^m\;Y_{i,k|k+1} \tag{33}$$

$$\hat{P}_{yy} = \sum_{i=0}^{2n} W_i^c \ (Y_{i,k|k+1} - \bar{y}_{k|k+1})(Y_{i,k|k+1} - \bar{y}_{k|k+1})^T \tag{34}$$

$$P_{yy} = \hat{P}_{yy} + R_k \tag{35}$$

$$P_{xy} = \sum_{i=0}^{2n} W_i^c \ (\hat{\chi}_{i,k|k+1} - \hat{x}_{k|k+1})(Y_{i,k|k+1} - \bar{y}_{k|k+1})^T \tag{36}$$

$$K_k = \ P_{xy} \ P_{yy}^{-1} \tag{37}$$

$$\hat{x}_k = \hat{x}_{k|k+1} + \ K_k \left(\ Y_k - \bar{y}_{k|k+1} \right) \tag{38}$$

$$P_k = \ P_{k|k+1} - \ K_k \ P_{yy} \ K_k^T \tag{39}$$

If the prior statistics of the noise are not known or change over time, an adaptive algorithm can be used. In this study, the statistical estimator is based on the reference [11], which is applied as follows. An estimate of the innovation covariance is obtained by averaging the innovation sequence over a window of length N

$$\hat{C}_v = \frac{1}{N} \sum_{j=k-N+1}^{k} \Delta\hat{x}_k \Delta\hat{x}_k^T \tag{40}$$

Then based on the whiteness of the filter innovation sequence the statistical matrices can be estimated as

$$\hat{R}_k = \hat{C}_v + \ P_{k|k+1} - \ K_{k+1} \ P_{yy} \ K_{k+1}{}^T \tag{41}$$

$$\hat{Q}_k = K_{k+1} \hat{C}_v K_{k+1}^T \tag{42}$$

The unscented Kalman filter's computational load is proportional to the number of sigma points which is related to the number of states. The following new minimum sigma sets $n+1$ were based on the reference [13].

$$W_0 = \frac{\kappa}{n+\kappa} \tag{43}$$

$$\alpha = \sqrt{\frac{1-W_0}{n}} \tag{44}$$

$$C = \sqrt{I_n - \alpha^2 1_n} \tag{45}$$

where $0 < W_0 < 1$.

The new sigma points are obtained by

$$\hat{\chi}_0 = \hat{x}_{k+1} - \frac{\sqrt{(n+\kappa)\, P_{(k+1)i}}}{\sqrt{W_0}} [\alpha]_{n\times 1} \tag{46}$$

$$\hat{\chi}_{i,k+1} = \hat{x}_{k+1} + \sqrt{(n+\kappa)\, P_{(k+1)i}} CISW_i, \qquad \forall i = 1, 2, ..., n \tag{47}$$

where ISW_i is the Cholesky decomposition of $diag(W_0 \alpha^2 C^{-1} 1_n (C^T)^{-1})$.

The design of this new AUKF is similar to the existing AUKF. Eqs. 29, 33, 34 and 36 have to be rewritten with the new defined weights:

$$\bar{y}_{k|k+1} = \sum_{i=0}^{n} \bar{W}_i \ Y_{i,k|k+1} \tag{48}$$

$$\hat{P}_{yy} = \sum_{i=0}^{n} \bar{W}_i \ (Y_{i,k|k+1} - \bar{y}_{k|k+1})(Y_{i,k|k+1} - \bar{y}_{k|k+1})^T \tag{49}$$

$$P_{yy} = \hat{P}_{yy} + R_k \tag{50}$$

$$P_{xy} = \sum_{i=0}^{n} \bar{W}_i \ (\hat{\chi}_{i,k|k+1} - \hat{x}_{k|k+1})(Y_{i,k|k+1} - \bar{y}_{k|k+1})^T \tag{51}$$

$\bar{W}_i$ is defined with the following equation:

$$\begin{bmatrix} \bar{W}1 & ... & \sqrt{\bar{W}_1}\sqrt{\bar{W}_n} \\ ... & ... & ... \\ \sqrt{\bar{W}_1}\sqrt{\bar{W}_n} & ... & \bar{W}_n \end{bmatrix} = W_0 \alpha^2 C^{-1} 1_n (C^T)^{-1} \tag{52}$$

Remark: Adaptations of R and Q are not performed simultaneously since these two values rely on each other when the covariance matching technique is used [19]. R is known since it is related to the sensor noise. If system faults occur, an adaptation on R might be performed [20].

VI. Simulation Results

The proposed reduced-set AUKF was studied in comparison with the existing AUKF and applied for the air bearing testing of a 1U CubeSat ADCS [14]. In our paper [14], the angular velocity estimated value had been compared with an existing AUKF and a reduced-set AUKF. The estimation of the new AUKF was faster and had better accuracy. The gyro drift estimation using the reduced-set AUKF and the existing AUKF showed the existing AUKF estimation errors were larger than that of the reduced-set AUKF. It can be seen that new AUKF was a better choice for a non-symmetric prior distributions for rate estimation. In this paper, we will only present the Euler Angles' estimation due to limited space.

A. Pure Magnetic Control using Only Three Magnetic Rods

This section presents the simulation results of applying the novel AUKF for satellite attitude parameter estimation. The system's dynamic equations use parameters $(J_1, J_2, J_3) = diag(0.02; 0.02; 0.007) kgm^2$ from the initial orientation and angular velocity of $(q_1, q_2, q_3, a_4) = (0.1, -0.1, 0.1, 0.8)$ and $(\omega_1, \omega_2, \omega_3) = (0.05, 0.05, 0.05) rad/s$. The maximum allowable magnetic dipole M=0.3 Am^2 is considered. In the first stage, the parameters of the control law are $H = diag([0.06e+6; 0.06e+6; 0.06e+6])$. In the second stage, the parameters of the control law are $H = ndiag([0.07e+6; 0.07e+6; 0.07e+6])$ and $A = diag([(0.9e+6)/400; (0.9e+6)/400; (0.9e+6)/400])$. The satellite is in

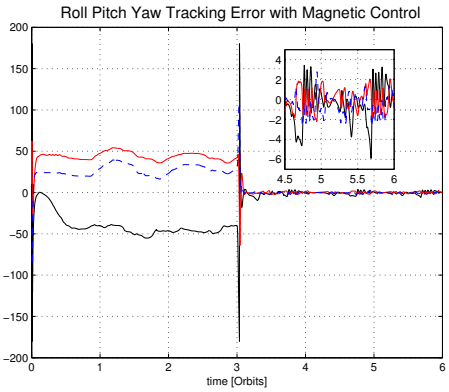

Fig. 2. 3U CubeSat Euler Angles Tracking Errors with Pure Magnetic Control in Six Orbits

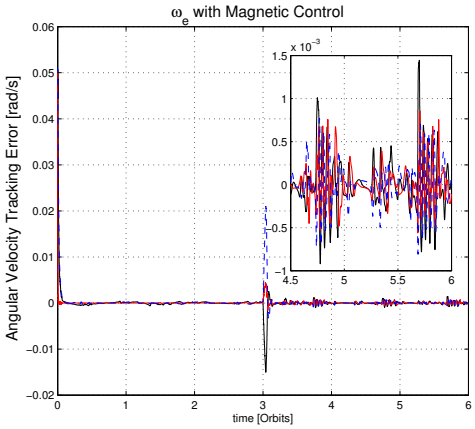

Fig. 3. 3U CubeSat Angular Velocity Tracking Errors with Pure Magnetic Control in Six Orbits

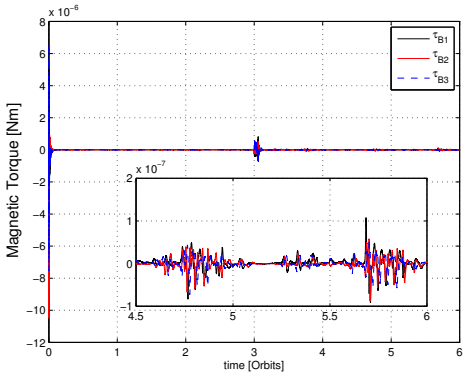

Fig. 4. 3U CubeSat Control Torques with Pure Magnetic Control in Six Orbits

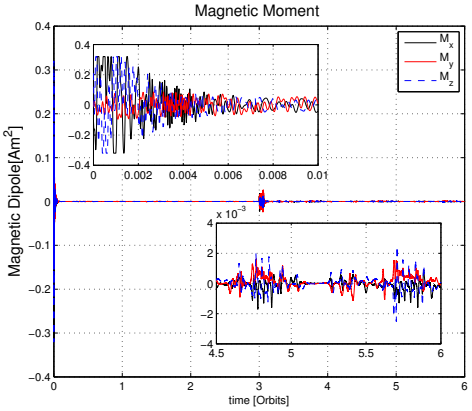

Fig. 5. 3U CubeSat Magnetic Dipoles with Pure Magnetic Control in Six Orbits

a 600 km orbit with inclination $i = 45$ degrees. The initial estimation values: process, measurement noise covariance matrices and initial sigma points are $R = diag([2e-8; 2e-8; 2e-8])$, $Q = diag([1e-15; 1e-15; 1e-15])$, and $p_0 = diag([1; 1; 1])$.

Figs. 2-6 show Euler angle tracking errors, angular velocity tracking errors, control torques and magnetic dipole results and AUKF estimation results of the system with three magnetic rods as actuators in 6 orbits of time. The angular velocity tracking errors are within $1.5e-3$ rad/s in 0.01 orbits. This is the damping mode of the satellite. At 3 orbits, we use another magnetic control law. We also started a nadir tracking mode. The attitude tracking accuracy is within 5 $degrees$. In Fig. 6, the AUKF estimated Euler roll angle is shown. The ADS is active after 3 orbits. The solid line is the actual value. The dashed line is the estimated value from the AUKF. The proposed $n+1$ AUKF computational load is much smaller than that of $2n+1$ sigma point UKF.

B. Hybrid Magnetic Control using Three Magnetic Rods and One Wheel

The nanosatellite is assumed to be a three axis stabilized body in a 600 km circular orbit with 45 degree inclination. The system's dynamic equations use parameters $(J_1, J_2, J_3) = diag(0.02; 0.02; 0.007)kgm^2$ from the initial orientation and angular velocity of $(q_1, q_2, q_3, a_4) = (0.1, -0.1, 0.1, 0.8)$ and $(\omega_1, \omega_2, \omega_3) = (0.0001, 0.0001, 0.0001)rad/s$. Figs. 7-9 show the Euler angle tracking errors, magnetic torques, and the estimated Euler Angles. The nadir pointing accuracy is within $5e-3$ degrees.

VII. Conclusion

In this research, the nonlinear attitude estimation and control system for a 3U nanosatellite has been validated using simulation results. The proposed new adaptive unscented Kalman filter was able to achieve estimation performance with $n+1$ sigma points. The proposed ADCS has successfully achieved detumbling and nadir pointing phases for a 3U nanosatellite. In upcoming work, we will verify the proposed magnetic control systems on nanosatellite attitude determination and control hardware using an air bearing system with a Helmholtz magnetic cage to provide an external field.

References

[1] Xiang, T., Meng, T., Wang, H., Han, K., and Jin, Z. H., "Design and n-orbit Performance of the Attitude Determinatin and Control System

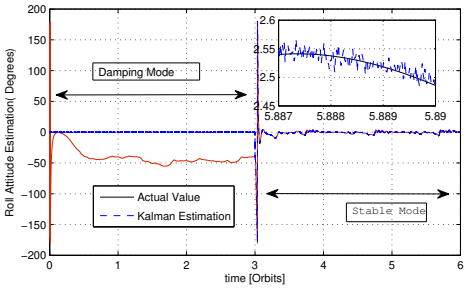

Fig. 6. 3U CubeSat AUKF Roll Estimation in Six Orbits

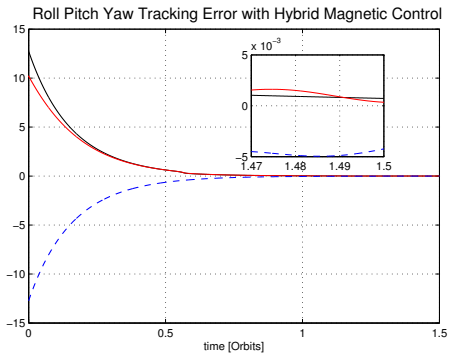

Fig. 7. 3U CubeSat Euler Angle Tracking Errors with Hybrid Magnetic Control in One and a Half Orbits

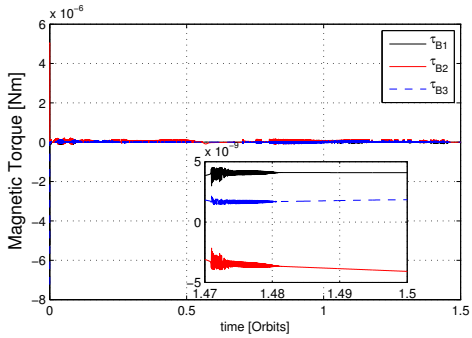

Fig. 8. 3U CubeSat Magnetic Torque with Hybrid Magnetic Control in One and a Half Orbits

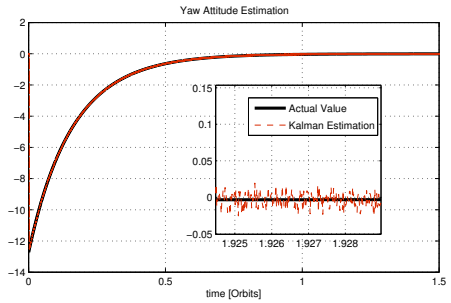

Fig. 9. 3U CubeSat Yaw Angle AUKF Estimation in One and a Half Orbits

for the ZDPS-1A Pico-satellite," *Acta Astronautica*, Vol. 77, 2012, pp. 182–196.

[2] Sekhavat, P., Gong, Q., and Ross, I. M., "NPSAT1 Parameter Estimation using Unscented Kalman Filtering," *Proceedings of the 2007 American Control Conference*, New York, USA, July 11- 13, 2007, FrA07.5.

[3] Silani, E. and Lovera, M., "Magnetic Spacecraft Attitude Control: A Survery and Some New Results," *Control Engineering Practice*, Vol. 13, 2005, pp. 357–371.

[4] Zhaowei, S., Xu, Y., and Di, Y., "Active Magnetic Control Methods for Small Satellite," *Journal of Aerospace Engineering*, Vol. 16, No. 1, 2003, pp. 38–44.

[5] Wisniewski, R., *Satellite Attitude Control using only Electromagnetic Actuation*, Dept. Control Eng. Aalborg University, Aalborg, 1996.

[6] Psiaki, M. L., "Magnetic Torquer Attitude Control via Asymptoic Periodic Linear Quadratic Regulation," *Journal of Guidance, Control and Dynamics*, Vol. 24, No. 2, 2001, pp. 386–394.

[7] Crassidis, J. L., Markley, F. L., and Cheng, Y., "Survey of Nonlinear Attitude Estimation Methods," *Journal of Guidance Control and Dynamics*, Vol. 30, No. 1, 2007, pp. 12–28.

[8] Leeghim, H., Choi, Y., and Jaroux, B. A., "Uncorrelated Unscented Filtering for Spacecraft Attitude Determination," *Acta Astronautica*, Vol. 67, 2010, pp. 135–144.

[9] Abdelrahman, M. and Park, S. Y., "Sigma-Point Kalman Filtering for Spacecraft Attitude and Rate Estimation using Magnetometer Measurements," *IEEE Transactions on Aerospace and Electronic Systems*, Vol. 47, No. 2, 2011, pp. 1401–1415.

[10] Soken, H. E. and Hajiyev, C., "UKF-Based Recofigurable Attitude Parameters Estimation and Magnetometer Calibration," *IEEE Transactions on Aerospace and Electronic Systems*, Vol. 48, No. 3, 2012, pp. 2614–2627.

[11] Vepa, R., "Ambulatory Position Tracking of Prosthetic Limbs using Multiple Satellite Aided Ineritial Sensors and Adaptive Mixing," *The Journal of Navigation*, Vol. 64, 2011, pp. 295–310.

[12] Bae, J. H. and Kim, Y. D., "Attitude Estimation for Satellite Fault Tolerant System using Federated Unscented Kalman Filter," *International Journal of Aeronautical and Space Science*, Vol. 11, No. 2, 2010, pp. 80–86.

[13] Menegaz, H. M., Ishihara, J. Y., and Borges, G. A., "A New Smallest Sigma Set for the Unscented Transform and its Applications on SLAM," *2011 50th IEEE Conference on Decision and Control and European Control Conference, Orlando, Fl, USA*, 2011, pp. 3172–3177.

[14] Post, M. A., Li, J., and Lee, R., "Nanosatellite Air Bearing Tests of Fault-Tolerant Sliding-Mode Attitude Control with Unscented Kalman Filter," *AIAA Guidance, Navigation, and Control Conference*, Minneapolis, Minnesota, August. 13-16, 2012.

[15] Lovera, M. and Astolfi., A., "Spacecraft Attitude Control using Magnetic Actuators," *Automatica*, Vol. 40, No. 8, 2004, pp. 1405–1414.

[16] Sofyal, A. and Jafarov, E. M., "Purely Magnetic Spacecraft Attitude Control by Using Classical and Modified Sliding Mode Algorithms," *12th IEEE Workshop on Variable Structure Systems,VS S12, January 12-14, Mumbai, 2012.*

[17] Wisniewski, R. and Blanke, M., "Fully Magnetic Attitude Control for Spacecraft Subject to Gravity Gradient," *Automatica*, Vol. 35, No. 7, 1999, pp. 1201–1204.

[18] Li, J. and Kumar, K. D., "Fault Tolerant Attitude Synchronization Control during Formation Flying," *Journal of Aerospace Engineering*, Vol. 24, 2011, pp. 251–263.

[19] Almagbile, A., Wang, J., and Ding, W., "Evaluating the Performances of Adaptive Kalman Filter Methods in GPS/INS Integration," *Journal of Global Positioning Systems*, Vol. 9, No. 1, 2010, pp. 33–40.

[20] Soken, H. E. and Hajiyev, C., "Pico Satellite Attitude Estimation via Robust Unscented Kalman Filter in the Presence of Measurement Faults," *ISA Transactions*, Vol. 49, No. 3, 2012, pp. 249–256.